Theoretical analysis of x-ray absorption spectra of Ti compounds used as catalysts in lithium amide/imide reactions

Takao Tsumuraya, Tatsuya Shishidou, and Tamio Oguchi*
Department of Quantum Matter, ADSM, Hiroshima University, 1-3-1 Kagamiyama, Higashi-Hiroshima, 739-8530, Japan
(Received 26 April 2008; published 18 June 2008)

We present a theoretical analysis and interpretation of the x-ray absorption near-edge structure of x-ray absorption spectroscopy (XAS) at the titanium *K*-edge of several Ti compounds for understanding catalysis mechanism in lithium amide $LiNH_2$ and imide Li_2NH systems for hydrogen storage. Our theoretical approach is based on first-principles calculations using all-electron full-potential linear augmented plane-wave method. Chemical bonding and local geometry of catalytically-active Ti states in the hydrogen desorption reaction $LiNH_2+LiH \rightarrow Li_2NH+H_2$ are investigated. It is found that XAS spectra of some compounds consisting of elements Li, N, H, and Ti are quite similar to measured ones of catalytically-active Ti compounds. We conclude that Ti ions may occupy the Li sites in $LiNH_2$ during the reaction.

DOI: 10.1103/PhysRevB.77.235114 PACS number(s): 71.15.Mb, 78.70.Dm, 71.20.Ps

I. INTRODUCTION

The safe and reliable hydrogen storage technologies are currently a major challenge to realize the future hydrogen economy. Solid-state storage is an efficient approach for this purpose. Here, high gravimetric density of hydrogen and low operation temperature are critical factors for the development of onboard vehicular hydrogen storage. Systems with light elements have attracted much attention due to their high gravimetric density of hydrogen. Chen *et al.* have originally focused on compounds composed of lithium, nitrogen, and hydrogen and reported that lithium nitride Li_3N can absorb hydrogen in the two-step reaction:[1]

$$Li_3N + 2H_2 \overset{\text{(i)}}{\leftrightarrow} Li_2NH + LiH + H_2 \overset{\text{(ii)}}{\leftrightarrow} LiNH_2 + 2LiH. \quad (1)$$

The reaction proceeds reversibly through gaseous hydrogen cycling between lithium amide $LiNH_2$ and lithium imide Li_2NH without any catalyst. Theoretically, 10.4 mass% of hydrogen can be reversibly stored in this reaction. Ichikawa *et al.* have studied the second step reaction (ii) since 6.5 mass% of hydrogen can be desorbed/absorbed due to smaller enthalpy change.[2] They have explored various transition-metal compounds as catalysts to improve the hydrogen absorption and desorption kinetics with a ball-milling technique. It has been found that a small amount (1 mol%) of some titanium additives affects the rate of a hydrogen desorption process in reaction (ii).[3,4] Ti particle clusters,[5] $TiCl_3$, and TiO_2 particles with an average diameter of 9 nm in anatase structure accelerate the H-desorption rate and slightly decrease the H-desorption temperature. On the other hand, Ti metal and TiO_2 with an average diameter of 10–100 μm show no clear catalytic effect. However, these catalysis mechanisms and the role of Ti in the reaction remain unknown.

X-ray absorption spectroscopy (XAS) is widely used to investigate the electronic states associated with particular element and symmetry. X-ray absorption near-edge structure (XANES) refers to the region of XAS spectra within about 40 eV above the absorption edge. This region contains information about chemical bonding and local geometry of atoms involved in the x-ray absorption transition.[6–8] Therefore, XAS is a valuable tool for investigating a local structure in complex materials such as ball-milled samples for hydrogen storage.[9,10] Isobe *et al.* have recently performed XAS measurements at the Ti *K*-edge for elucidating the catalysis mechanism in the reaction (ii).[11] Results of the XAS measurements clearly show that Ti compounds which have a catalytic effect on the kinetics of H-desorption share a common spectrum shape near the edge observed during reaction (ii). This indicates that the Ti ions are situated in a specific local geometry and chemical bonding state in the reaction. However, little is known about the local structure and bonding nature associated with the common spectrum shape.

In this paper, we present a theoretical analysis and interpretation of the near-edge structure of XAS at the Ti *K*-edge of several related compounds from first principles. We calculate theoretical XAS spectra of Ti metal and compounds to compare them with the measured spectra and provide several important information about the origin of the XAS spectra. We discuss the possible origin of the common near-edge structure by analyzing chemical bonding and local structure around Ti in a catalytically-active state.

II. METHODS

The present first-principles calculations are based on the density functional theory by adopting the all-electron full-potential linear augmented plane-wave (FLAPW) method.[12–14] Exchange and correlation are treated within local density approximation (LDA) (Ref. 15) or generalized gradient approximation (GGA).[16] LDA and GGA gave almost identical electronic structure and XAS spectra for a given crystal structure. We show only LDA results below. One-electron Kohn-Sham equations are solved self-consistently with scalar relativistic scheme and improved tetrahedron method is used for the Brillouin-zone integration with the k mesh $16\times16\times16$ for TiO, TiN, and TiH_2, $14\times14\times14$ for Ti metal and TiO_2, $12\times12\times12$ for $TiCl_3$, $3\times3\times3$ for Li_3TiN_2, $4\times4\times4$ for $Li_7Ti(NH)_4$, and $6\times6\times6$ for $Li_3Ti(NH_2)_4$. Muffin-tin sphere radii are set to be 0.9 Å for Ti and Cl, 0.8 Å for O and Li, 0.6 Å for N, and

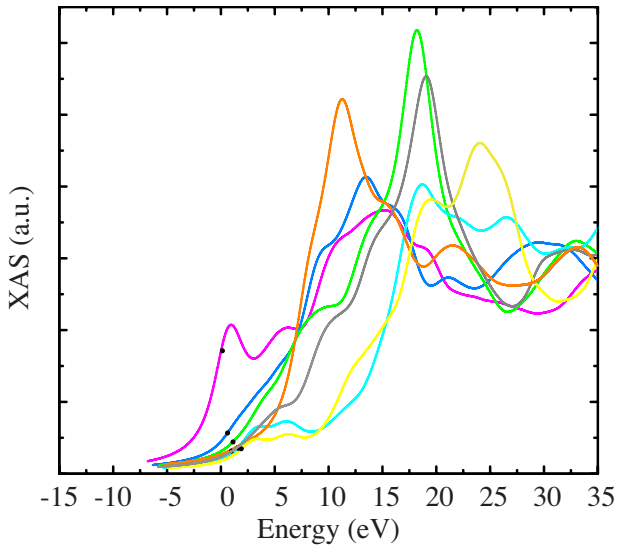

FIG. 1. (Color online) Theoretical XAS spectra at the Ti *K*-edge in reference samples, Ti metal (purple line), TiH_2 (blue), TiO (green), TiN (gray), $TiCl_3$ (orange), TiO_2 in anatase structure (sky blue), and TiO_2 in rutile structure (yellow). The origin of energy is set as the threshold of Ti metal. A black dot on each spectrum refers to the threshold for each compound.

0.35 Å for H. The cutoffs are 20 and 80 Ry for the LAPW basis and the potential and charge density, respectively. The implementation of the FLAPW method includes total energy and atomic-force calculations, which allows structural optimization.

XAS spectra are calculated by the following scheme. The probability of transition per unit time is written by Fermi's golden rule as

$$I(\omega) = \frac{2\pi}{\hbar} \sum_f |\langle f|\hat{F}|i\rangle|^2 \delta(\epsilon_i + \hbar\omega - \epsilon_f), \tag{2}$$

where ϵ_i and ϵ_f are the eigen energies of the initial $|i\rangle$ and final $|f\rangle$ states, respectively, and $\langle f|\hat{F}|i\rangle$ is the matrix element of the perturbation due to the interaction with photon. Here, the dipole approximation is used. The operator $\hat{F}$ can be written as

$$\hat{F} = e\mathbf{E} \cdot \mathbf{r} = e(E_x x + E_y y + E_z z), \tag{3}$$

where $\mathbf{E}$ and $\mathbf{r}$ are a photon electric field vector and an electron coordinate, respectively. For comparison with experiments, unpolarized light with all three terms in Eq. (2) is assumed. In the present study, we investigate the Ti *K*-edge, where the initial state is the Ti 1*s* core state and the final state is unoccupied bands with *p* symmetry around the Ti site. Since the initial state is a highly localized core state, the transition matrix elements are calculated only within the Ti muffin-tin sphere. All the theoretical spectra are broadened by a Lorentzian function $L(\omega) = \frac{1}{\pi}\frac{\Delta}{\Delta^2+\omega^2}$ with $\Delta = 1.5$ eV for the sake of comparison with experiment. We also estimate the influence of core shift for spectra. The core shift corresponds to the differences in photo-threshold of the XAS spectrum, which is defined as the Fermi energy in a metallic system or the conduction band bottom in case of an insulator (such as TiO_2) minus the Ti 1*s* core level.

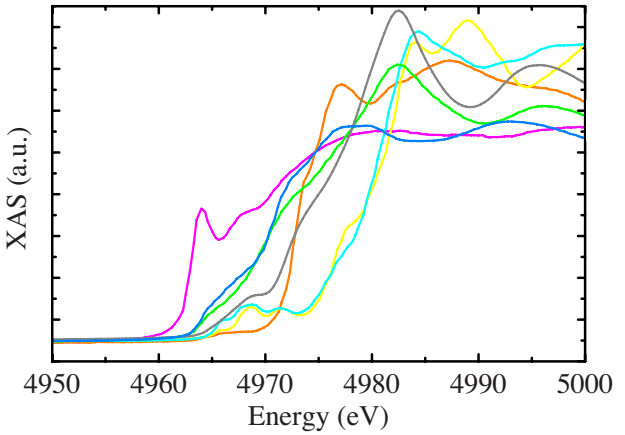

FIG. 2. (Color online) Measured XAS spectra at the Ti *K*-edge of reference samples, Ti metal (purple line), TiH_2 (blue), TiO (green), TiN (gray), $TiCl_3$ (orange), TiO_2 in anatase structure (sky blue), and TiO_2 in rutile structure (yellow), after Ref. 11.

III. RESULTS AND DISCUSSION

A. Reference materials

For understanding the bonding nature and local geometry of catalytically-active states, it is quite useful to study reference materials first since their crystal structure and stoichiometric composition are well identified. We obtain theoretical XAS spectra for several reference materials as shown in Fig. 1. The experimental spectra measured by Isobe *et al.*[11] are depicted in Fig. 2. Generally, the calculated spectrum agrees well with the measured one. We used the experimental lattice data determined by x-ray diffraction, as listed in Table I. As the XAS spectra indicate, the spectrum shape is unique for each compound. Ti metal has a large pre-edge in the energy region of 0–3 eV. The $TiCl_3$ spectrum suddenly rises up within 5 eV. TiH_2 shows a main structure around 12 eV. The spectra of TiO and TiN have main structures between 15 and 20 eV with the broad edge structure. TiO_2 in anatase and rutile structures reveals a main structure in the high photon-energy region and two small pre-edge structures. In the

TABLE I. Crystal structure of Ti compounds as reference samples which were determined experimentally (Ref. 28).

	Space group	*a* (Å)	*c* (Å)
Ti metal	$P6_3/mmc$	2.905	4.683
TiH_2	$Fm\bar{3}m$	4.44	
TiO	$Fm\bar{3}m$	4.177	
TiN	$Fm\bar{3}m$	4.24	
$TiCl_3$	$P6_3/mcm$	6.27	5.82
TiO_2 anatase	$I4_1/amd$	3.759	9.514
TiO_2 rutile	$P4_2/mnm$	4.59	2.96

TABLE II. Calculated core shift to be observed as a change in the absorption threshold.

	Valence	Core shift (eV)
Ti metal	0	0
TiH_2	2	0.478
TiO	2	1.105
TiN	3	0.977
$TiCl_3$	3	1.602
TiO_2	4	1.611

present study, we discuss the origin of spectrum shape via the overall feature of the measured spectra and its relation to local structure and bonding nature by analyzing the electronic structure.

XAS is the direct observation of electronic states involved in the relevant electronic transition. The electric dipole transitions are known to be dominant in the Ti *K*-edge XAS, though some features from electric quadrupole transitions have been found in the pre-edge structure.[17,18] In the Ti *K*-edge XAS spectra, there are two factors that determine the spectrum shape. One is core shift, also called chemical shift, that is given by the energy difference of the initial state of the transition, namely the Ti 1*s* core level, among the compounds. The core shift does not affect the shape of the spectrum but determines the position of the photo-threshold. Some experimental XAS reports have claimed that the near-edge structures are usually interpreted in terms of the Ti formal valence.[10,11] Graetz *et al.*[10] have reported that the 13 eV-difference in the onset of the main structure between Ti metal and TiO_2 is attributed to the chemical shift by their different Ti valences. Our estimations of the core shift are summarized in Table II. As a result, we have found theoretically that the core shift is quite small, at most 2 eV. Therefore, the 13 eV-difference cannot be understood by only the core shift. The other factor is the density of the final states with *p* symmetry. Figure 3 shows the calculated partial electronic density of states (DOS) of the unoccupied *p*-states for Ti metal and compounds. The Ti-*p* components of DOS are clearly reflected in the spectrum features. For transition metals, the partial *p* DOS is remarkably affected by hybridization with surrounding orbitals since the wave functions of the *p*-state are extended. The *K*-edge spectrum is a useful tool to get information of the chemical bonding and local geometry around the atom involved in the transition. Now, we shall take a close look at the relation between electronic structure and local structure of each compound for understanding the spectra.

1. Ti metal

The crystal structure of titanium metal is hexagonal ($P6_3/mmc$) with two Ti atoms in the unit cell. Figure 1 presents our calculated XAS spectrum of Ti metal, together with those of Ti compounds. The unoccupied partial *p* DOS is shown in Fig. 3(a). The Ti *p*-states are significantly hybridized with the *d*-state of the neighboring Ti atoms. The large

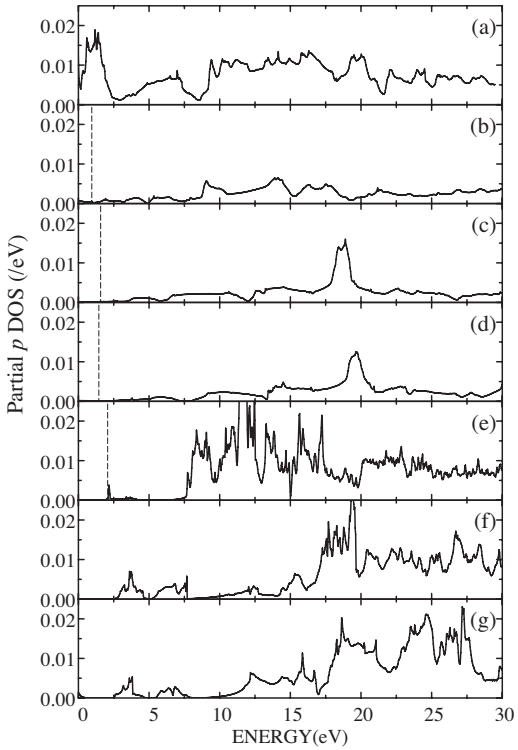

FIG. 3. Calculated partial *p*-density of states (DOS) of Ti metal and its compounds. (a) Ti metal, (b) TiH_2, (c) TiO, (d) TiN, (e) $TiCl_3$, (f) TiO_2 in anatase structure, and (g) TiO_2 in rutile structure. A vertical dashed line represents the threshold for each metallic material. The energy zero is set as the Fermi energy of Ti metal.

pre-edge structure originates from the bonding state between the *p* orbitals of a Ti atom and the *d* orbitals of its neighboring sites while the main structure comes from their antibonding counterparts. There is a pseudogap in the partial *p* DOS around 2–3 eV above the Fermi energy, called "antiresonance" that roughly indicates the border between the bonding and antibonding states.

2. $TiCl_3$

Titanium trichloride is hexagonal and its space group is $P6_3/mcm$ with lattice constants $a=6.27$ and $c=5.82$ Å with four $TiCl_3$ f.u./unit cell. The unoccupied partial *p* DOS is shown in Fig. 3(e). There is a steep acclivity between 5 and 10 eV in the XAS spectrum as one can see in Fig. 1. The main structure is located in a lower energy region compared to the oxides and nitride, implying a less covalent and more ionic nature. The nearest-neighbor atoms of Ti are six Cl at a distance of 2.45 Å and the second nearest-neighbor atoms are two Ti at 2.91 Å. Ti-*p* states are hybridized mostly with Cl-*s* and *p*, less hybridized with Ti *d* states around the Fermi energy though Cl-*p* states are hybridized with Ti *d*-states. Thus, there is almost few state in the partial *p* DOS between 0 and 5 eV.

3. TiH_2, TiO and TiN

For titanium dihydride TiH_2, monoxide TiO and nitride TiN, the unoccupied partial *p* DOS's are depicted in Figs.

3(b)–3(d). These materials share a face-centered cubic crystal structure (space group $Fm\bar{3}m$) with a lattice constant of 4.44 Å for TiH_2, 4.18 Å for TiO, and 4.24 Å for TiN. A Ti atom is coordinated by six O (N) in TiO (TiN) and eight H in TiH_2. The monoxide and nitride show a main peak in the high photon-energy region with relatively small pre-edge structure. The main structure arises from the antibonding state between the Ti p and the neighboring anion s and p orbitals. Due to similar degree in the covalent nature in the monoxide and nitride, the main structures are located around 15–20 eV above the threshold. The main structure of TiH_2 is located in a slightly lower energy region compared to TiO and TiN, since the degree of covalency becomes weaker.

4. TiO_2

Anatase TiO_2 has a tetragonal structure with the space group $I4_1/amd$ and lattice constants $a=3.759$ and $c=9.514$ Å. Rutile TiO_2 has a tetragonal structure ($P4_2/mnm$) with lattice constants $a=4.59$ and $c=2.96$ Å. In both structures, the primitive unit cell contains two Ti and four O ions. In the rutile structure, a Ti ion is coordinated octahedrally by six O ions with the same Ti-O bond lengths, while in anatase structure, it is coordinated nearly octahedrally by six O ions with two different Ti-O bond lengths. The theoretical XAS spectra of both structures have two pre-edge structures in the low energy region around 0–8 eV and the main structure is located in the high-energy region around 18–20 eV above the threshold as shown in Fig. 1. It is noted that the intensity of the pre-edge structure in anatase is slightly larger than that in rutile. The pre-edge structures are interpreted as being the result of mixing of Ti-p onto the antibonding state between Ti-d and O-p in the conduction band bottom as can be seen from the analysis of unoccupied partial p DOS in Figs. 3(f) and 3(g). It should be noted that the point group of the Ti site in the anatase structure is $\bar{4}m2$ and allows on-site hybridization between the Ti-p and d orbitals due to lack of inversion symmetry. This on-site hybridization may lead to enhancement of the pre-edge structure in the K-edge spectrum. Actually, we have found a less pronounced pre-edge structure for rutile TiO_2, where inversion symmetry is retained. However, the enhancement in the pre-edge structure of anatase TiO_2 is not so significant because the local coordination of O ions around Ti is close to that with inversion symmetry. This tells that the pre-edge structure may be a clue to interpret the local structure of Ti compound with or without inversion symmetry. In the measured spectra for anatase and rutile, a quite small but well defined peak can be seen around 4965 eV in Fig. 2, but our calculated spectra of both TiO_2 show no such peak. The XAS spectra have been calculated by a tight-binding linear muffin-tin orbital band-structure method[19] and full-potential cluster calculation based on the finite difference method.[17] Joly *et al.*[17] and Uozumi *et al.*[20] discussed the contribution of quadrupole transition in both structures of TiO_2 and concluded that the lowest-energy peak comes from a quadrupolar transition to t_{2g} orbitals coupled with influence of the core hole effect. The peak cannot be observed in our spectrum since our calculations have been performed within the electric dipole approximation. We are now in progress to estimate the contribution of quadrupole transition to the XAS spectra by implementing it into our first-principles method.

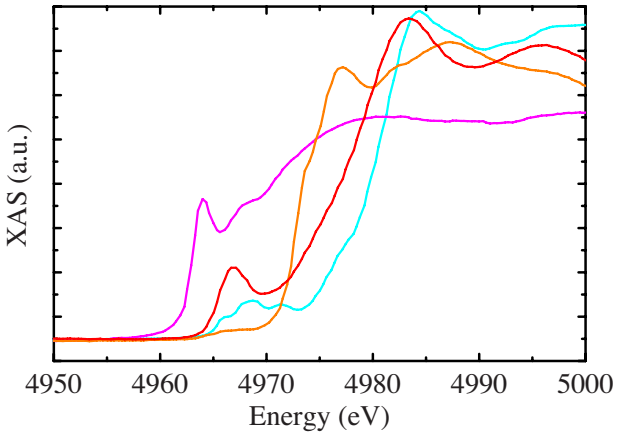

FIG. 4. (Color online) Measured spectra at the Ti K-edge for the composites with $LiNH_2$ and LiH catalyzed by $TiCl_3$ (red line) and the reference sample of $TiCl_3$ (orange), Ti metal (purple), and TiO_2 in anatase structure (sky blue).

B. Reactions involving $LiNH_2$, LiH and Ti compounds

1. Experimental background

The analysis of experimental XAS spectra is usually performed by a simple comparison with spectra of reference samples as a fingerprint matching. As indicated in the results of XAS measurements by Isobe *et al.*,[11] the catalytically-active Ti compounds have a common spectrum shape near the edge, while the other compounds show different shapes. For instance, the common spectrum of catalytically-active $TiCl_3$ in the reaction (ii) is depicted in Fig. 4. The spectrum has a prominent pre-edge structure between 4965 and 4970 eV and the main structure is located in a higher energy region. However, no spectrum of the reference samples discussed above corresponds to spectrum shape with catalytically-active state. In other words, the local structure and bonding nature of Ti might be changed during the hydrogen desorption reaction.

2. Candidate compound with the common spectrum shape

In the catalytically-active Ti state, the prominent pre-edge structure can be seen in the measured XAS spectrum, indicating a relatively large hybridization of the Ti p-state with neighboring d orbitals as in Ti metal and the dioxides shown above (see Fig. 4). In addition, the enhancement of the p-component of the partial DOS in the pre-edge energy region may include on-site hybridization with d orbitals due to the noncentrosymmetric point group at the Ti site. Then, among compounds with the elements Li, N, H, and Ti, we explore a compound showing such an enhanced pre-edge structure. First, we find Li_5TiN_3 as a candidate. We have performed calculations of the electronic structure for this compound based on the crystal structure reported by Juza *et al.*[21] Note that the stoichiometry of our calculated structure is

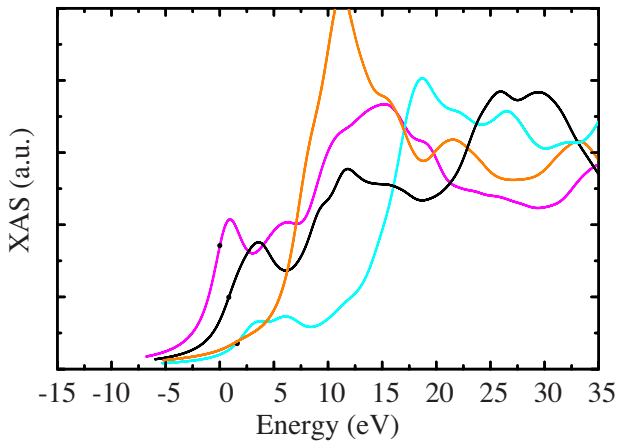

FIG. 5. (Color online) Theoretical spectra at the Ti *K*-edge for Li_3TiN_2 (black line) and the reference samples of $TiCl_3$ (orange), Ti metal (purple), and TIO_2 in anatase structure (sky blue). A black dot on each spectrum refers to the threshold for each compound.

Li_3TiN_2 since the 16*c* site is assumed to be Ti but the local structure around Ti remains equivalent. Our calculated spectrum for Li_3TiN_2 is illustrated in Fig. 5. As a result, a reasonable agreement is obtained between theoretical and experimental XAS spectra around the pre-edge region, but the main structure does not show such a good correspondence with the measured spectrum. The calculated main structure is situated in a somewhat lower photon energy compared to the experimentally observed one. One important thing to note is that the crystal structure of Li_5TiN_3 is significantly similar to that of Li_2NH (Ref. 22) and $LiNH_2$. The most interesting common feature is that the Ti sites in Li_3TiN_2 and the Li sites in Li_2NH and $LiNH_2$ are tetrahedrally coordinated by N. The neighboring atom coordinations are listed in Table III. In order to further investigate the clear pre-edge structure, we discuss the electronic structure of Li_3TiN_2. Figure 8(c) shows the unoccupied partial *p* DOS. The origin of the pre-edge structure can be interpreted as resulting from the mixing of Ti-*p* onto the antibonding state between $d(t_{2g})$ orbitals of the off-site Ti and N-*s* and *p*. In addition, it can be

TABLE III. The number of neighboring atoms around the Ti site in Li_3TiN_2 and the Li site in Li_2NH and $LiNH_2$.

		N	N	Li	Li	H	H
Li_3TiN_2 [a]	Distance (Å)	2.008	2.014	2.520	2.560		
	Number	3	1	3	3		
Li_2NH [b]	Distance (Å)	2.040		2.506		3.016	
	Number	4		4		4	
$LiNH_2$ [c]	Distance (Å)	2.066		2.515		2.355	2.945
	Number	4		4		4	4

[a]Reference 21.
[b]Reference 22.
[c]Reference 23.

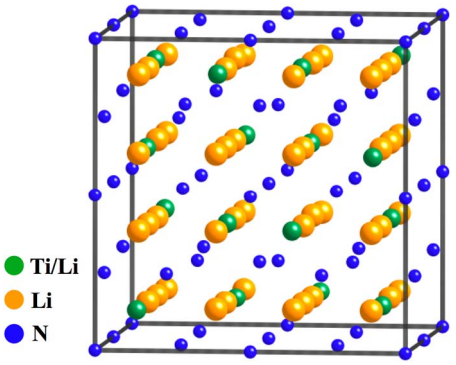

FIG. 6. (Color online) Crystal structure of Li_5TiN_3 experimentally determined by Juza *et al.* (Ref. 21). The space group is $Ia\bar{3}$ (No.206). The lattice constant $a=9.7$ Å. The green atoms represent 16*c* site (x,x,x) with $x=0.12$, of which two thirds and one third are occupied by Ti and Li, respectively. All of the 16*c* sites are assumed to be Ti in the present calculation.

expected that Ti-*p* states have large hybridization with the on-site *d* orbitals because of the lack of centrosymmetry.

3. Ti substitution for Li sites of $LiNH_2$ and Li_2NH

In the crystal structure of Li_5TiN_3 (Fig. 6), the Li and N framework resembles that in $LiNH_2$ and Li_2NH. The cation (Li) sites in $LiNH_2$ and Li_2NH are also tetrahedrally coordinated by N. Therefore, we expect that replacing the Li site with Ti in $LiNH_2$ and Li_2NH will result in a similar prominent pre-edge structure. The crystal structure of $LiNH_2$ is tetragonal $(I\bar{4},Z=8)$.[23] The lattice constants are taken from the optimized results by our FLAPW calculation.[24] We assume that one of the four Li sites is substituted by Ti. So, the stoichiometry of this virtual compound is $Li_3Ti(NH_2)_4$. For the crystal structure of Li_2NH, we employ the orthorhombic *Ima*2 structure determined by Herbst *et al.*[25] In the structure, we assume that one of the eight Li sites of Li_2NH is substituted by Ti. Therefore, the resultant stoichiometry is $Li_7Ti(NH)_4$. Calculated XAS spectra for these two compounds are shown in Fig. 7. These spectra also have a clear pre-edge structure as that of the spectrum of Li_3TiN_2. The peak position and general feature between the spectra of $Li_7Ti(NH)_4$ and Li_3TiN_2 are almost the same, while the main structure of $Li_3Ti(NH_2)_4$ is located in the high-energy region around 18 eV. Among the three candidate Ti compounds, the near-edge structure of $Li_3Ti(NH_2)_4$ is the closest to the experimentally observed one. The unoccupied *p* partial DOS of $Li_3Ti(NH_2)_4$ and $Li_7Ti(NH)_4$ are shown in Figs. 8(a) and 8(b), respectively. From the analysis of these partial DOS, we conclude that the origin of the clear pre-edge structure are the antibonding states due to the large hybridization with Ti-*d* as in Li_3TiN_2. The fact that the Ti site is tetrahedrally coordinated by N is important to introduce the enhanced pre-edge structure in these compounds.

C. Reaction mechanism

By taking the present and previous results into consideration, we can make the following remarks on the reaction

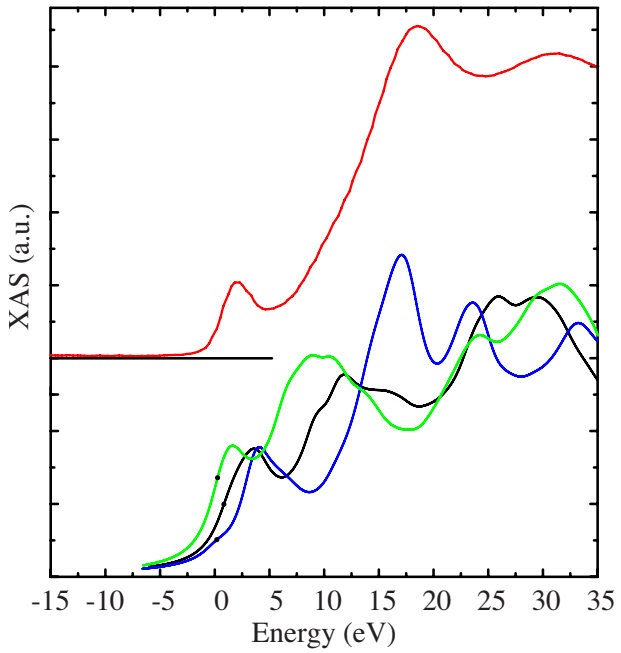

FIG. 7. (Color online) Theoretical spectra at Ti *K*-edge for $Li_7Ti(NH)_4$ (light green line), $Li_3Ti(NH_2)_4$ (blue), and Li_3TiN_2 (black). A black dot on each spectrum refers to the threshold for each compound. The red line represents the measured spectrum of the composites with $LiNH_2$ and LiH catalyzed by $TiCl_3$.

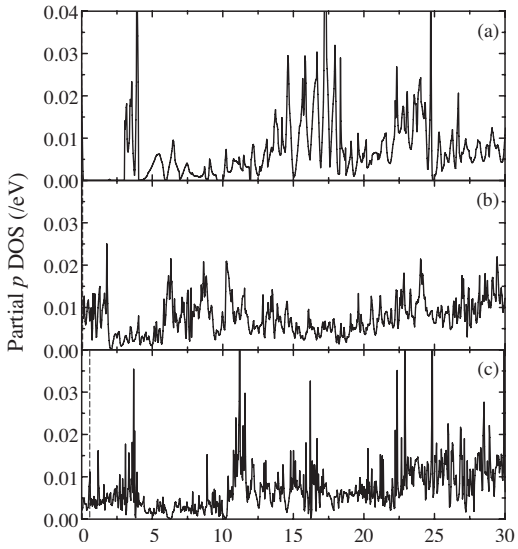

FIG. 8. Calculated partial *p*-density of states of Ti compounds. (a) $Li_3Ti(NH_2)_4$, (b) $Li_7Ti(NH)_4$, (c) Li_3TiN_2. The threshold is represented by a dashed line for each material. The energy zero is set as the Fermi energy of $Li_3Ti(NH_2)_4$.

mechanisms. From the results of the crystal structure determination[22,23,26,27] in the amide-imide systems, the common feature of the crystal structures of Li_2NH, $LiNH_2$, $Mg(NH_2)_2$, and $Li_2Mg(NH)_2$ is that nitrogen is basically located at the pseudo face-centered cubic position. Therefore, the N skeleton is retained during hydrogenation and dehydrogenation, while the Li and H ions might be mobile during the reactions. From the discussion in the preceding section, we conclude that Ti ions may occupy the Li sites in ball-milled $LiNH_2$ and Li_2NH samples with active Ti catalysts.

IV. CONCLUSION

We presented the theoretical XAS spectra and electronic structure of Ti metal and compounds from first-principles calculations using the FLAPW method. It is found that XAS at the Ti *K*-edge reflects mostly the empty extended *p* states hybridized with states surrounding the Ti ions, and that the core shifts play no important role. In Ti compounds, the general feature of the spectra is due to the antibonding state between the Ti-*p* and the neighboring anion *s* and *p* orbitals. We studied the local structure of measured spectra of catalytically-active states. It is found that the spectrum shape of Li_3TiN_2 has the prominent pre-edge structure, as seen in the common spectrum shape in the catalytically-active Ti state. The common structural feature in Li_3TiN_2, Li_2NH, and $LiNH_2$ is that Ti in Li_3TiN_2 and Li in Li_2NH and $LiNH_2$ are tetrahedrally coordinated by N. The enhancement in the pre-edge structure is attributed to the on-site hybridization between Ti-*p* and Ti-*d* due to the lack of centrosymmetry realized in the tetrahedrally coordinated structure. We expect that Ti ions may occupy the Li sites in $LiNH_2$ in catalytically-active states during the reaction.

ACKNOWLEDGMENTS

This work was supported in part by the Grants of the NEDO project "Advanced Fundamental Research on Hydrogen Storage Materials." The computation in this work was partly performed using the facilities of the Supercomputer Center at Institute for Solid State Physics, University of Tokyo. We thank Shigehito Isobe, Satoshi Hino, Hiroki Miyaoka, Takayuki Ichikawa, Nobuko Hanada, Yoshitsugu Kojima, and Hironobu Fujii for invaluable discussions.

*oguchi@hiroshima-u.ac.jp

[1] P. Chen, Z. Xiong, J. Luo, J. Lin, and K. L Tan, Nature (London) **420**, 302 (2002).
[2] T. Ichikawa, S. Isobe, N. Hanada, and H. Fujii, J. Alloys Compd. **365**, 271 (2004).
[3] T. Ichikawa, N. Hanada, S. Isobe, H. Leng, and H. Fujii, J. Alloys Compd. **404-406**, 435 (2005).
[4] S. Isobe, T. Ichikawa, N. Hanada, H. Leng, M. Fichtner, O. Fuhr, and H. Fujii, J. Alloys Compd. **404-406**, 439 (2005).
[5] M. Fichtner, O. Fuhr, O. Kircher, and J. Rothe, Nanotechnology **14**, 778 (2003).
[6] L. A. Grunes, Phys. Rev. B **27**, 2111 (1983).
[7] F. Farges, G. E. Brown, and J. J. Rehr, Phys. Rev. B **56**, 1809 (1997).

[8] N. Jiang, D. Su, and J. C. H. Spence, Phys. Rev. B **76**, 214117 (2007).
[9] N. Hanada, T. Ichikawa, and H. Fujii, Physica B **383**, 49 (2006).
[10] J. Graetz, J. J. Reilly, J. Johnson, A. Y. Ignatov, and T. A. Tyson, Appl. Phys. Lett. **85**, 500 (2004).
[11] S. Isobe, T. Ichikawa, Y. Kojima, and H. Fujii, J. Alloys Compd. **446-447**, 360 (2007).
[12] E. Wimmer, H. Krakauer, M. Weinert, and A. J. Freeman, Phys. Rev. B **24**, 864 (1981).
[13] J. M. Soler and A. R. Williams, Phys. Rev. B **40**, 1560 (1989).
[14] M. Weinert, J. Math. Phys. **22**, 2433 (1981).
[15] J. F. Janak, V. L. Moruzzi, and A. R. Williams, Phys. Rev. B **12**, 1257 (1975).
[16] J. P. Perdew, K. Burke, and M. Ernzerhof, Phys. Rev. Lett. **77**, 3865 (1996).
[17] Y. Joly, D. Cabaret, H. Renevier, and C. R. Natoli, Phys. Rev. Lett. **82**, 2398 (1999).
[18] M. Takahashi, J. Igarashi, and P. Fulde, J. Phys. Soc. Jpn. **69**, 1614 (2000).
[19] Z. Y. Wu, G. Ouvrard, P. Gressier, and C. R. Natoli, Phys. Rev. B **55**, 10382 (1997).
[20] T. Uozumi, K. Okada, A. Kotani, O. Durmeyer, J. P. Kappler, E. Beaurepaire, and J. C. Parlebas, Europhys. Lett. **18**, 85 (1992).
[21] R. Juza, H. H. Weber, and E. Meyer-Simon, Z. Anorg. Allg. Chem. **273**, 48 (1953).
[22] M. P. Balogh, C. Y. Jones, J. Herbst, L. G. Hector, Jr., and M. Kundrat, J. Alloys Compd. **420**, 326 (2006).
[23] M. H. Sørby, Y. Nakamura, H. W. Bricks, S. Hino, H. Fujii, and B. C. Hauback, J. Alloys Compd. **428**, 297 (2007).
[24] T. Tsumuraya, T. Shishidou, and T. Oguchi, J. Alloys Compd. **446-447**, 323 (2007).
[25] J. F. Herbst and L. G. Hector, Jr., Phys. Rev. B **72**, 125120 (2005).
[26] J. Rijssenbeek, Y. Gao, J. Hanson, Q. Huang, C. Jones, and B. Toby, J. Alloys Compd. **454**, 233 (2008).
[27] W. I. F. David, M. Jones, D. Gregory, C. Jewell, S. Johnson, A. Walton, and P. Edwards, J. Am. Chem. Soc. **129**, 1594 (2007).
[28] P. Villars and D. L. Calvert, *Pearson's Handbook of Crystallographic Data for Intermetallic Phases, Desk Edition* (American Society for Metals, Metals Park, OH, 1997).